Tracking the pre-clinical progression of transthyretin amyloid cardiomyopathy using artificial intelligence-enabled electrocardiography and echocardiography

Evangelos K. Oikonomou MD DPhil[a,b], Veer Sangha BS[b,c], Sumukh Vasisht Shankar MS[a,b], Andreas Coppi PhD[b,d], Harlan M. Krumholz MD SM[a,d], Khurram Nasir MD MPH,[e,f,g] Edward J. Miller MD PhD[a], Cesia Gallegos-Kattan MD MHS[a], Mouaz H. Al-Mallah MD MSc[g], Sadeer Al-Kindi MD[g,h], Rohan Khera MD MS[a,b,d,i,j*]

[a] Section of Cardiovascular Medicine, Department of Internal Medicine, Yale School of Medicine, New Haven, CT, USA

[b] Cardiovascular Data Science (CarDS) Lab, Yale School of Medicine, New Haven, CT, USA

[c] Department of Engineering Science, University of Oxford, Oxford, UK

[d] Center for Outcomes Research and Evaluation, Yale-New Haven Hospital, New Haven, CT, USA

[e] Division of Cardiovascular Prevention and Wellness, Department of Cardiology, Houston Methodist DeBakey Heart & Vascular Center, Houston, TX

[f] Houston Methodist-Rice Digital Health Institute, Houston, TX, USA

[g] Houston Methodist DeBakey Heart and Vascular Center, Houston, TX, USA

[h] Center for Cardiovascular Computational & Precision Health, Houston Methodist DeBakey Heart & Vascular Center, Houston, TX, USA

[i] Section of Biomedical Informatics and Data Science, Yale School of Medicine, New Haven, CT, USA

[j] Section of Health Informatics, Department of Biostatistics, Yale School of Public Health, New Haven, CT, USA

Manuscript type: Original Research Manuscript

Brief title: AI for pre-clinical transthyretin amyloid cardiomyopathy

Word count: 3,893 words**; Figures:** 4**; Tables:** 2

[*]**Correspondence to:** Rohan Khera, MD, MS

195 Church St, 6th Floor, New Haven, CT 06510

203-764-5885; rohan.khera@yale.edu

ABSTRACT

Background and Aims: The diagnosis of transthyretin amyloid cardiomyopathy (ATTR-CM) requires advanced imaging, precluding large-scale testing for pre-clinical disease. We examined an application of artificial intelligence (AI) to transthoracic echocardiography (TTE) and electrocardiography (ECG) as a scalable risk stratification strategy for pre-clinical ATTR-CM.

Methods: In age/sex-matched case-control datasets in the Yale-New Haven Health System (YNHHS) we trained deep learning models to identify ATTR-CM-specific signatures on TTE videos and ECG images (area under the curve of 0.93 and 0.91, respectively). We deployed these across studies of individuals referred for nuclear cardiac amyloid testing in an independent population at YNHHS and an external population from Houston Methodist Hospitals (HMH). We evaluated longitudinal trends in AI-defined probabilities of ATTR-CM using age/sex-adjusted linear mixed models and their ability to stratify the risk of ATTR-CM across pre-clinical stages.

Results: Among 984 participants at YNHHS (median age 74 years, 44.3% female) and 806 at HMH (69 years, 34.5% female), 112 (11.4%) and 174 (21.6%) tested positive for ATTR-CM, respectively. Across cohorts and modalities, AI-defined ATTR-CM probabilities derived from 7,423 TTEs and 32,205 ECGs diverged as early as 3 years before clinical diagnosis in cases versus controls ($p_{\text{time(x)group interaction}} \leq 0.004$). One-to-three years *before* referral for ATTR-CM testing, a double-negative screen (AI-Echo(-)/AI-ECG(-)) had sensitivity of 0.98 (95%CI:0.96-0.99) and 0.89 (95%CI:0.86-0.92), whereas a double-positive screen (AI-Echo(+)/AI-ECG(+)) yielded specificity of 0.72 (95%CI:0.69-0.74) and 0.91 (95%CI:0.90-0.91) in YNHHS and HMH, respectively.

Conclusions: AI applied to echocardiographic videos and ECG images may enable scalable risk stratification of ATTR-CM during its early pre-clinical course.

Keywords: cardiac amyloidosis, transthyretin, artificial intelligence, screening, echocardiography, electrocardiography

GRAPHICAL ABSTRACT

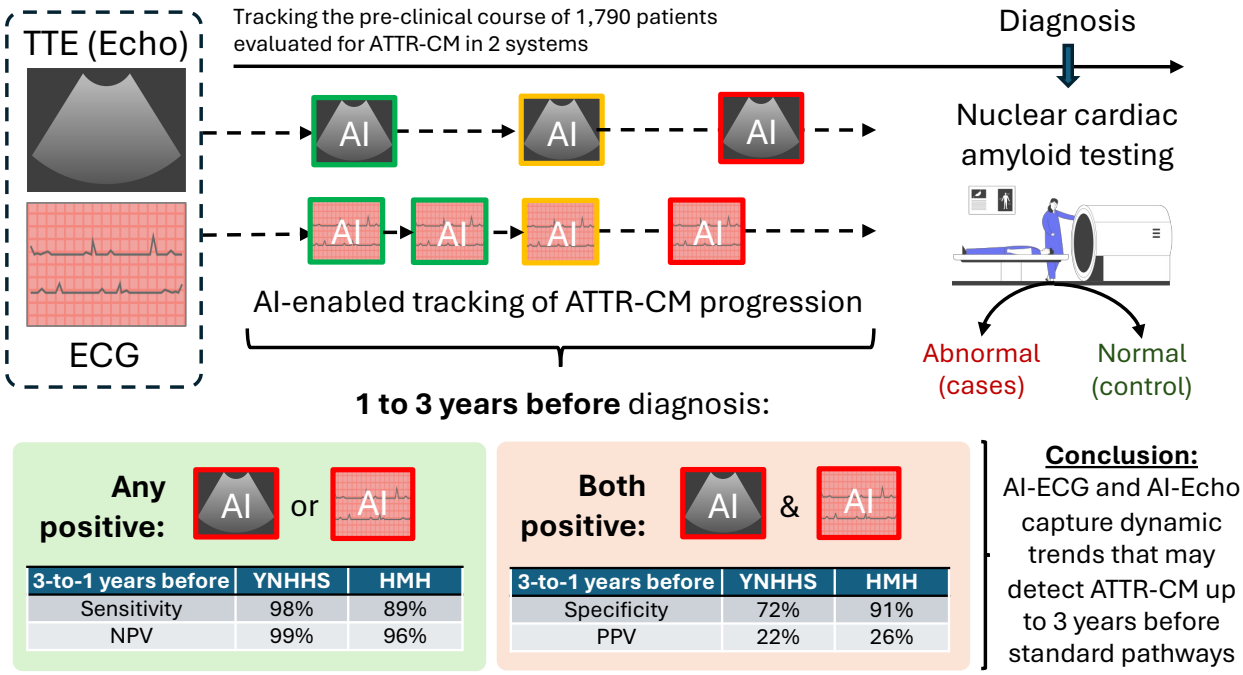

Key question: Can artificial intelligence (AI) applied to transthoracic echocardiography (TTE) and electrocardiographic (ECG) images detect transthyretin amyloid cardiomyopathy (ATTR-CM) early in its pre-clinical course?

Key finding: Across 1,790 patients referred for nuclear cardiac amyloid imaging in two large and diverse hospital systems, AI-Echo and AI-ECG probabilities for ATTR-CM may be used independently or in conjunction to screen for ATTR-CM 1-to-3 years before diagnosis is established through traditional pathways.

Take-home message: AI applied directly to echocardiography and ECG images may define a scalable paradigm in the monitoring of pre-clinical ATTR-CM progression and help identify candidates who may benefit from initiation of disease-modifying therapies.

INTRODUCTION

Awareness of the insidious onset and progression of transthyretin amyloid cardiomyopathy (ATTR-CM) is increasing, with growing recognition of its under-appreciated prevalence and links to incident heart failure and premature mortality.[1–6] This is partly due to the evolution of several new therapeutic agents that can effectively reduce the associated morbidity and mortality.[7–9] These therapies can stabilize abnormally folded transthyretin protein that deposits in myocardium,[8,9] silence its production,[9–11] and even promote its clearance,[12] thereby modifying the course of the disease, especially when deployed early during the disease course.[13] Despite these advances, on-treatment mortality and morbidity remain high,[7,8,13] suggesting the need for earlier identification and treatment. The key challenge with optimizing the use of these new therapeutic agents is identifying individuals before the onset of symptoms, long before traditional diagnostic testing is usually performed. While dedicated nuclear cardiac amyloid testing remains a key part of the diagnostic cascade,[1,14] the need for access to specialized centers, its cost, and radiation exposure, may limit its broader use in identifying those with pre-clinical disease. Therefore, there are currently no scalable strategies or tools to identify individuals with pre-clinical disease and track its progression to flag the appropriate time for intervention.

In this study, we hypothesized that structural, electrical, and mechanical changes induced by the deposition of amyloid fibrils are detectable through AI-enhanced interpretation of routine transthoracic echocardiography (TTE) and 12-lead electrocardiography (ECG) long before the development of clinical disease and its recognition, thus offering a scalable strategy for the early identification of pre-clinical ATTR-CM. Using a multi-center cohort of individuals referred for ATTR-CM evaluation, both with and without a confirmed diagnosis, we aimed to characterize longitudinal trajectories of quantitative AI-Echo and AI-ECG phenotypes and their performance

as stand-alone or combined tests in distinguishing cases from controls during the years preceding diagnosis (**Figure 1**).

METHODS

Study overview and data source

This was a retrospective study across two large and diverse health systems, namely the Yale-New Haven Health System (YNHHS, internal set), spanning 5 hospitals and affiliated clinic sites across Connecticut and Rhode Island, and the geographically distinct Houston Methodist Hospitals (HMH, external testing set, with 8 hospitals and affiliated clinic sites) in Houston, Texas. We followed a two-stage analytical approach. First, we trained independent AI-Echo and AI-ECG models to discriminate cases of ATTR-CM from age/sex-matched controls in YNHHS, thus learning the distinct echocardiographic and ECG signature of the ATTR-CM phenotype. Second, we deployed these models across all serial TTEs and ECGs performed in independent sets of individuals referred for nuclear cardiac amyloid testing in YNHHS (internal testing) and HMH (external testing). All individuals were 18 years or older at the time of their exam. This design allowed us to assess the temporal evolution of AI-Echo and AI-ECG probabilities and their utility in discriminating future disease in the years before nuclear cardiac amyloid testing (**Figure 2**).[15] Respective Institutional Review Boards approved the study protocol and waived the need for informed consent as the study involves secondary analysis of pre-existing data.

Study definitions

To train an AI-Echo and AI-ECG classifier for the cross-sectional detection of ATTR-CM, we defined any TTE or ECG studies performed up to one year before or any time after an abnormal

nuclear cardiac amyloid study as positive for the ATTR-CM phenotype. This definition ensured the specificity of the label for ATTR-CM and was based on the median delay (latency) in ATTR-CM diagnosis that has been estimated at 12-13 months across contemporary studies.[13,16] Across cohorts, nuclear cardiac amyloid testing was performed in accordance with the recommendations of the American Society of Nuclear Cardiology using single photon emission tomography-computed tomography [SPECT-CT] imaging with Tc^{99m}-pyrophosphate [PYP] or other approved radiotracer. The final diagnosis of a positive study was adjudicated by the interpreting physician based on semi-quantitative visual grading (grade ≥2), or a heart-to-contralateral lung ratio of >1.5, where applicable.[15] Clinical risk factors, co-morbidities and amyloidosis-related codes were extract by querying the respective EHR up to 12 months after the nuclear cardiac amyloidosis study (**Table S1**).

Development cohorts: learning cross-sectional signatures of ATTR-CM

AI-Echo model development

AI-Echo training population: Given the lower counts of echocardiograms relative to ECG studies and to ensure that patients with sequential studies were not seen during model training, participants who had ≥2 TTE studies before a nuclear cardiac amyloid exam were not included in the training or validation of the amyloid detection models, but were reserved for the progression analysis. The diagnostic model development population included 308 studies from 101 unique individuals, split at a patient level into training and validation sets (80%, 20%) to develop an AI-Echo model for detecting concurrent ATTR-CM. Age- and sex-matched controls (10 controls per case) were sampled from individuals from the same period without a history of abnormal nuclear

cardiac amyloid imaging or an ICD amyloidosis code specific for transthyretin amyloidosis ("E85.82"). The AI-Echo model development population is summarized in **Table S2**.

AI-Echo model training: We followed our previously described end-to-end pre-processing pipeline for echocardiographic studies stored in DICOM (Digital Imaging and Communications in Medicine) format, which involves deidentification, automated view classification steps, as well as standard augmentation by padding, random rotation, and horizontal flipping.[17] We used a 3D ResNet-18 backbone, class-balanced loss function (weighted binary cross-entropy), the Adam optimizer, a learning rate of 10^{-4}, a batch size of 56, a random dropout of 0.25, and label smoothing (α of 0.1), and trained our algorithm for a maximum of 30 epochs with patience (early stopping) set at 5 epochs. For predictive estimates for the full echocardiographic study, we used key echocardiographic views that included the left ventricle and left atrium (parasternal long axis, and any of the standard apical four-, three- or two-chamber views) as inputs and performed mean averaging of the output probabilities across these views. The full process is described in the **Supplement**.

AI-ECG model development

AI-ECG training population: The AI-ECG image model was trained in line with our previously described approach,[18–20] and is also described separately.[21] To increase the accuracy of our labels, we required that all controls had a TTE performed ≤15 days of the ECG during training but did not receive a diagnosis of ATTR-CM during follow-up. The AI-ECG development population is summarized in **Table S3**.

AI-ECG model training: Images of ECGs were generated from 12-lead recordings at a frequency of 500 Hz for 10 seconds collected on various machines (i.e., Philips PageWriter machines and GE MAC machines). We followed our previously described approach of standard transformation, calibration, plotting across various lead layout formats, baseline wander correction, and random augmentation.[18] We used an EfficientNet-B3 backbone that was initialized using weights from a self-supervised biometric contrastive learning approach that we have previously defined.[19] We used a class-balanced binary cross-entropy loss function, an Adam optimizer, gradient clipping, a learning rate of 64, a batch size of 10^{-5}. The full process and training population is described in the **Supplement**.

Testing cohorts: evaluating pre-clinical ATTR-CM progression by AI-Echo & AI-ECG

The trained models were independently deployed across two geographically distinct patient populations drawn from YNHHS (September 2016 through January 2024: *internal testing cohort*) and HMH (March 2016 through May 2024: *external testing cohort*). The presence of two geographically distinct cohorts enabled a more robust assessment of performance across institutions and populations with different baseline risk and referral patterns. For the ECG analysis at YNHHS, we removed samples that had previously been used during the model's training. We stratified both the YNHHS and HMH cohorts based on the results of the nuclear cardiac amyloid test as positive (first positive study for any individuals eventually diagnosed with ATTR-CM) or negative (first negative study, with no established diagnosis by the end of follow-up). Negative nuclear cardiac amyloid studies represented the controls since clinical suspicion was high enough to prompt referral for dedicated nuclear imaging. We directly deployed the AI-Echo and AI-ECG models to all TTE videos and ECG images from these

participants (done before or after their nuclear cardiac amyloid test). Across cohorts, all TTE studies were available in standard DICOM format. In YNHHS (internal testing), ECG images were available in a standard format as .png files, whereas in HMH (external testing), these were exported directly as flattened .pdf files. To ensure transparency during testing in an external population, we embedded both the AI-ECG and AI-Echo models into executable applications that contained standardized environments and enabled direct inference on the TTE and ECG studies at HMH. The software applications can be made available upon reasonable request as part of a research collaboration. Interactive applications for both algorithms are openly available on our website for research use with deidentified data (see data availability statement).

Statistical analysis

Continuous variables are presented as median [25th-75th percentile] and compared using the Mann-Whitney test across two groups. Categorical variables are summarized as counts (and percentages) and compared across distinct groups using the χ^2 test. During training, we summarized the discrimination performance of the AI-Echo and AI-ECG models using the area under the receiver operating characteristic curve [AUROC] for ATTR-CM with corresponding 95% confidence intervals (CI) derived from bootstrapping with 1,000 replications.

To assess the differential progression in AI-Echo and AI-ECG output probabilities (0 to 1) for the ATTR-CM phenotype across nuclear cardiac amyloid testing-positive vs negative participants, we fit a mixed-effects linear regression model with the AI-Echo or AI-ECG probability of ATTR-CM as the dependent variable, and the following fixed effects: nuclear cardiac amyloid imaging status (positive versus negative), the time difference between each ECG/TTE study, their interaction term, the time of nuclear cardiac amyloid imaging, age at the

time of nuclear cardiac amyloid imaging, and sex. Given the correlatedness of observations within the same subject, participant was included as a random effect. Summary statistics (means and 95% confidence interval of mean) were also estimated and summarized across discrete time intervals (more than 5 years before nuclear cardiac amyloid imaging, 3 to 5 years before, 1 to 3 years before, last 12 months, or any time after). Furthermore, we derived annualized progression rates in the dependent variable (AI probability of ATTR-CM) across cases and controls by extracting the coefficients (and respective standard errors) for time and its interaction with nuclear cardiac amyloid imaging status from the previously fitted mixed linear model.

Finally, we examined the ability of AI-Echo and AI-ECG to independently or jointly discriminate future ATTR-CM across these distinct time intervals. We present patient-level discrimination metrics (sensitivity, specificity, positive, negative predictive value) at a fixed "sensitive" threshold of 0.015 (but also across thresholds of 0.05, 0.10, 0.25, and 0.50) for various approaches: i) AI-Echo alone, ii) AI-ECG alone, iii) AI-Echo OR AI-ECG screening ("Either" approach: ≥1 positive), and iv) AI-Echo AND AI-ECG screening ("Both" approach: requiring AI tests to be positive) (see **Supplement** on the modelling used). We provide 95% confidence intervals calculated by non-parametric bootstrapping with 1,000 replications. All statistical tests were two-sided with a significance level of 0.05 unless specified otherwise. All analyses were performed using Python version 3.11.2 (Python Software Foundation) and R version 4.2.3 (R Foundation).

RESULTS

Cross-sectional discrimination of ATTR-CM by AI-ECG and AI-Echo

We first confirmed the ability of AI-Echo and AI-ECG models to discriminate ATTR-CM. In the TTE held-out testing cohort that included 138 TTE cases and 1380 TTE control studies (median age 79 [IQR: 75, 84] years, 1166 [76.8%] male [**Table S2**]), the AI-Echo model reached a study-level AUROC of 0.93 (95%CI: 0.90-0.96). Similarly, in the ECG held-out testing cohort from YNHHS that included 139 ECG cases and 1390 ECG controls (median age 80 [IQR: 75, 86] years, 1,044 [68.3%] male [**Table S3**]) the AI-ECG model successfully discriminated ATTR-CM cases from controls with an AUROC of 0.91 (95%CI: 0.88-0.93).

Pre-clinical cohort analysis

The AI-Echo and AI-ECG models were independently deployed across the pre-clinical progression cohorts. There were 4,010 unique TTEs and 22,340 ECGs in 984 unique individuals in the progression cohort at YNHHS, with 112 of these individuals (11.4%) having abnormal findings compatible with ATTR-CM on nuclear cardiac amyloid testing. At the external site, HMH, there were 3,413 TTEs and 9,865 ECGs in 806 participants, with 174 (21.6%) eventually diagnosed with ATTR-CM. Compared with negative cases, positive cases were older at the time of nuclear cardiac amyloid imaging (YNHHS: 82 [IQR 75, 86] vs 73 [IQR 64, 80] years, and HMH: 77 [IQR 70, 82] vs 67 [IQR 57, 75] years, all $p<0.001$) and more frequently men (YNHHS: n=77 [68.8%] vs n=471 [54.0%], and HMH: n=145 [83.3%] vs n=383 [60.6%], $p<0.001$). Further differences in representative comorbidities across groups are summarized in **Table 1**.

Longitudinal phenotyping of the pre-clinical ATTR-CM phenotype by AI-Echo & AI-ECG

In the five years before nuclear cardiac amyloid testing was performed we observed a significant rise the AI-defined probabilities of ATTR-CM among those who went on to test positive by nuclear cardiac amyloid imaging compared with their counterparts, findings that were consistent across cohorts (YNHHS: internal testing; HMH: external testing) and modalities (TTE and ECG) (*study-level summary shown in* **Figure 3;** *participant-level summary shown in* **Figure S1**). Despite relative overlap in the AI probabilities >5 years before diagnosis between cases and controls, longitudinal follow-up demonstrated that the AI phenotypes started diverging as early as 3 years before diagnosis. In age- and sex-adjusted analyses in YNHHS, the annualized progression rate in AI-Echo probabilities was estimated at 2.3%/year [95%CI: 1.8%-2.9%/year] in cases vs 0.6%/year [95%CI: 0.5%-0.9%/year] in controls, and for AI-ECG at 1.5%/year [95%CI: 1.2%-1.7%/year] in cases vs 0.7%/year [95%CI: 0.6%-0.9%/year] in controls. These findings were replicated in the HMH cohort, with annualized progression rates of 1.8%/year [95%CI: 1.3%-2.3%] vs 0.3%/year [95%CI: 0.1-0.5%] for AI-Echo, and 1.8%/year [95%CI: 1.2-2.4%] vs 1.0% [95%CI: 0.7%-1.3%] for AI-ECG. Across all analyses, we observed a significant interaction when modelling nuclear cardiac amyloid testing positivity and time against AI-Echo and AI-ECG probabilities, thus supporting disproportionately faster progression rates among nuclear imaging-positive vs -negative cases in the years before diagnosis (**Table 2**). Of note, a subgroup analysis of confirmed cases of AL amyloidosis (n=19 [1.9%] individuals in YNHHS, and n=37 [4.6%] in HMH) suggests a similar rise in the year before nuclear cardiac amyloid testing both in YNHHS and HMH (**Figure S2**).

Diagnostic performance of AI-Echo and AI-ECG risk stratification for early ATTR-CM

Based on these observations, we evaluated the diagnostic performance of AI-Echo and AI-ECG, both as stand-alone tests and in combination, for discriminating ATTR-CM cases from controls across discrete time windows in the years preceding clinical diagnosis. **Figure 4** and **Table S4** summarize the evolution in discrimination metrics across different strategies (AI-Echo alone, AI-ECG alone, "Either" [at least one positive], or "Both" [both needed to be positive]), distinct pre-clinical time periods (3-5 years, 1-3 year, and up to 1 year before the nuclear cardiac amyloid exam), and AI-thresholds (1.5%, 5%, 10%, 25%, 50%). We find that across both the internal (YNHHS) and external (HMH) testing cohorts, up to 1-to-3 years *before* ATTR-CM testing, a double-negative screen (both AI-Echo(-) and AI-ECG(-)) had sensitivity of 0.98 (95%CI: 0.96-0.99) and 0.89 (95%CI: 0.86-0.92), with negative predictive value of 0.99 (95%CI: 0.98-0.99) and 0.96 (0.94-0.97), respectively. On the other hand, a double-positive screen (AI-Echo(+)/AI-ECG(+)) was associated with a specificity of 0.72 (95%CI: 0.69-0.74) and 0.91 (95%CI: 0.90-0.91), and positive predictive value of 0.22 (95%CI: 0.20-0.24) and 0.26 (95%CI: 0.23-0.29) across YNHHS and HMH, respectively.

DISCUSSION

In two large, diverse, and geographically distinct health system-based cohorts, we demonstrate that AI applied to standard TTE videos and ECG images enables scalable risk stratification and screening for ATTR-CM early in its course and before clinical diagnosis through standard pathways. Our findings introduce a new paradigm in which AI-enhanced interpretation of accessible diagnostic tests may be used to detect ATTR-associated changes which precede the clinical diagnosis of ATTR-CM by several years. We provide evidence to support the generalizability of these observations across distinct cohorts, and further illustrate their dynamic

nature in line with the natural history of ATTR-CM progression. These findings support the use of AI-Echo and AI-ECG in identifying at-risk individuals, guiding downstream diagnostics and informing the application of novel risk-modifying therapies while also enabling monitoring through cost-effective technologies.

Our findings should be interpreted in the context of recent evidence on the changing epidemiological and therapeutic landscape of ATTR-CM. Given advances in the non-invasive diagnosis by nuclear cardiac amyloid imaging and cardiac magnetic resonance (CMR) imaging, referrals to amyloidosis centers have been increasing.[13] While a U.K.-based study estimated that the median duration of symptoms prior to diagnosis has decreased from 36 months in 2002 to 12 months in 2021,[22] multinational registries demonstrate persistent delays from symptom onset to ATTR-CM diagnosis that often exceed two years.[22] There is also a growing recognition that myocardial ATTR deposition often co-exists with prevalent conditions, such as aortic stenosis and heart failure with preserved ejection fraction,[23] thus highlighting an emerging need for scalable and cost-efficient screening tool that can be deployed serially in at-risk populations.

To date, efforts to develop reliable prognostic biomarkers for ATTR-CM have been hampered by the low prevalence in the community, complex etiological and pathophysiological profile, and substantial heterogeneity across cases.[1] However, rapid advances in the therapeutic landscape of ATTR-CM have revealed a gap in scalable diagnostics to monitor the pre-clinical stages of the condition. Most prognostic markers have been evaluated among patients with an existing diagnosis, such as NT-proBNP (N-terminal pro-Brain Natriuretic Peptide) levels or outpatient intensification of diuretics, which consistently portend worse prognosis among patients with ATTR-CM.[24,25] Furthermore, while nuclear cardiac amyloid imaging represents an excellent non-invasive alternative to traditional biopsy,[26–28] it is expensive, not widely available,

and associated with radiation exposure, all features that preclude its use in longitudinal monitoring. Recently, attention has shifted to maximizing inference from easily scalable modalities performed during initial patient evaluation. AI methods directly applied to ECG signals and TTE videos have shown potential in detecting distinct electrical and structural signatures associated with the cardiac amyloidosis phenotype.[26–28] However, these models have been limited to individuals with established diagnosis and do not inform the use of these models in the risk stratification of preclinical ATTR-CM. Thus, our study introduces a novel role for AI-ECG and AI-Echo in the screening, risk stratification, and longitudinal disease monitoring of pre-clinical ATTR-CM through accessible and scalable biomarkers. Expanding AI-assisted phenotyping to the pre-clinical stages of ATTR-CM represents a critical unmet need to boost its timely recognition, monitor its progression, and eventually guide the deployment of disease-modifying therapies.[29]

As the potential eligibility pool for new therapies expands further, AI-enabled phenotyping could also guide optimal case selection during this pre-clinical stage and identify individuals who may derive the greatest benefit from early intervention based on an objectively quantifiable and dynamically evolving phenotype. Moreover, since many variant forms (i.e., V122I, pV142I) are more prevalent among traditionally disadvantaged communities, including racial and ethnic monitories (i.e., individuals of African or Hispanic/Latino ancestry), AI-enabled interpretation of accessible diagnostic modalities may also improve access to timely diagnostic care,[30–32] given that they represent the most commonly accessible form of ECGs available to the end-users. With the arrival of a rapidly expanding armamentarium of therapeutic agents that can not only stabilize abnormal TTR, but also inhibit its production in the liver and promote its clearance once deposited in remote organs,[1,7,8,10–12,33] AI-Echo and AI-ECG-enabled risk

stratification methods may identify at-risk individuals, guide targeted enrichment in prospective clinical trials, and further expand our knowledge on the pre-clinical stages of the disease, its trajectory, and the ability to modify it. This concept of early preventive intervention is already being explored in phase 3 trials of transthyretin stabilizers in individuals with pathogenic *TTR* variants, however assessment of response requires access to gold-standard nuclear cardiac amyloid imaging.[34]

Ultimately, our method may be applied both retrospectively and prospectively across repositories of cardiac diagnostics, as well as at the point of care, to identify, track, and risk stratify the earliest pre-clinical stages of ATTR-CM from accessible, widely available and inexpensive modalities. A sample implementation framework is summarized in **Figure S3**, although this would require prospective validation before integration into clinical pathways. Here, a double negative screen demonstrates a high NPV, potentially deferring the need for further testing, whereas a double-positive screen exhibits high specificity and PPV, enabling early identification of at-risk patients before clinical suspicion arises or nuclear cardiac amyloid testing is performed. Although the proposed strategy relies on single, one-time assessment, longitudinal monitoring with AI-Echo and AI-ECG could provide additional insights in equivocal cases or when clinical suspicion persists. By enabling longitudinal monitoring through standardized interpretation of scalable diagnostic modalities, our proposed strategy also enhances precision by minimizing rater variability and mitigating potential sources of referral and diagnostic bias associated with limited access to advanced imaging facilities.[35]

Limitations: Certain limitations merit consideration. First, this was a retrospective analysis of individuals in whom clinical suspicion for ATTR-CM prompted a referral for dedicated nuclear

cardiac amyloid testing. Similarly, ECG and TTE studies performed before or after clinical diagnosis were part of clinical care, thus introducing selection bias. As a result, it is unclear whether these findings can generalize to undiagnosed patients with pre-clinical ATTR-CM in the community who were never screened by ECG, TTE, or nuclear cardiac amyloid testing. Second, nuclear imaging-negative cases were younger and less likely to be male than their nuclear imaging-positive counterparts. Although the longitudinal trends were independent of age and sex, a negative study does not rule out the future development of the disease, particularly if testing was done at very early stages. Third, we relied on nuclear cardiac amyloid imaging with bone-avid radiotracers such as Tc^{99m}-PYP which are known to be highly sensitive and specific for ATTR-CM using established quantitative and semi-quantitative thresholds.[25] However, since these studies were performed as part of clinical care, there was no consistent multimodal assessment, or histological confirmation. Similarly, there was no consistent genotyping to assess differential trends across variant and wild-type forms of the disease. Fourth, our case definition allowed for some overlap forms of nuclear imaging-positive AL amyloidosis (possible AL/ATTR overlap) to be included in the cases and nuclear imaging-negative forms of non-ATTR (e.g. AL amyloidosis) to be included in the controls. This reflects the limitations of non-invasive imaging and the challenges of diagnosing cardiac amyloidosis. Nevertheless, subgroup analyses suggest that a similar, possibly steeper rise may emerge for individuals with AL amyloidosis, but this requires further investigation in dedicated studies. Fifth, ATTR-CM is a dynamic process, and a negative screen does not rule out future disease which may manifest several years later. In these cases, longitudinal monitoring of AI-derived probabilities may offer an observer-independent, quantitative metric to examine longitudinal changes. For screening purposes, however, decisions should likely rely on the most recent exam, rather than

retrospective, historical trends. Sixth, care practices may differ across centers, and the participants included in our analysis may have been evaluated by different teams of general practitioners, cardiologists, or cardiomyopathy specialists at different parts of their care, thus introducing potential heterogeneity in the cohorts. We also observed differences in demographics and the prevalence of abnormal nuclear cardiac amyloid test results across the internal and external testing cohorts, although this did not affect the validity of our observations. Ultimately, the broader paradigm suggested by this analysis requires further evaluation in prospective clinical cohorts or trials with protocolized imaging of at-risk populations.

CONCLUSIONS

AI technology applied directly to echocardiography and ECG images may enable scalable identification and risk stratification of pre-clinical ATTR-CM. These findings suggest a possible role for AI-enabled interpretation of routinely performed cardiac investigations to flag individuals at high risk of progressing to clinical ATTR-CM.

FUNDING

National Heart, Lung, and Blood Institute of the National Institutes of Health (under awards R01HL167858 and K23HL153775 to RK, and F32HL170592 to EKO), National Institute on Aging of the National Institutes of Health (under award number R01AG089981 to RK), Doris Duke Charitable Foundation (under award number 2022060 to RK), and BridgeBio (through funding awarded to RK through Yale University).

DISCLOSURE OF INTEREST

Dr. Oikonomou is a co-founder of Evidence2Health LLC, has been an ad hoc consultant for Ensight-AI Inc, and Caristo Diagnostics Ltd, a co-inventor in patent applications (18/813,882, 17/720,068, 63/508,315, 63/580,137, 63/619,241, 63/562,335 through Yale University) and patents (US12067714B2, US11948230B2 through the University of Oxford), and has received royalty fees from technology licensed through the University of Oxford outside this work. Dr. Sangha is a co-inventor of U.S. patent applications 63/428,569, 63/346,610, and 63/484,426, and co-founder of Ensight-AI Inc. Dr. Krumholz works under contract with the Centers for Medicare & Medicaid Services to support quality measurement programs, was a recipient of a research grant from Johnson & Johnson, through Yale University, to support clinical trial data sharing; was a recipient of a research agreement, through Yale University, from the Shenzhen Center for Health Information for work to advance intelligent disease prevention and health promotion; collaborates with the National Center for Cardiovascular Diseases in Beijing; receives payment from the Arnold & Porter Law Firm for work related to the Sanofi clopidogrel litigation, from the Martin Baughman Law Firm for work related to the Cook Celect IVC filter litigation, and from the Siegfried and Jensen Law Firm for work related to Vioxx litigation; chairs a Cardiac Scientific Advisory Board for UnitedHealth; was a member of the IBM Watson Health Life Sciences Board; is a member of the Advisory Board for Element Science, the Advisory Board for Facebook, and the Physician Advisory Board for Aetna; and is the co-founder of Hugo Health, a personal health information platform, and co-founder of Refactor Health, a healthcare AI-augmented data management company, and Ensight-AI, Inc. Dr. Gallegos-Kattan reports an educational grant (through Yale) and honoraria from Pfizer, and participation in advisory boards for AstraZeneca, BridgeBio and Pfizer. Dr. Miller is a consultant for Eidos, Pfizer, Siemens,

Alnylam, and Roivant; and has received grant support from Eidos, Pfizer, and Argospect. Dr. Nasir is on the advisory board of Novo Nordisk, Novartis, Amgen, Esperion, Merck Sharp and Dohme, and ER Squib & Sons, and discloses partial research support by grants from National Institutes of Health, Patient-Centered Outcomes Research Institute, Novartis, and Esperion. Dr. Khera is an Associate Editor of JAMA and receives research support, through Yale, from the Blavatnik Foundation, Bristol-Myers Squibb, Novo Nordisk, and BridgeBio. He is a coinventor of U.S. Patent Applications 63/177,117, 63/428,569, 63/346,610, 63/484,426, 63/508,315, 63/580,137, 63/606,203, 63/562,335, and a co-founder of Ensight-AI, Inc and Evidence2Health, LLC. All other authors declare no competing interests relevant to this manuscript.

DATA AVAILABILITY STATEMENT

The underlying data represent protected health information. To protect patient privacy, the local Institutional Review Boards within each center do not allow the sharing of these data. Browser-accessible interactive versions of the AI-Echo and AI-ECG models are openly available on our Lab's website for research use (AI-ECG: https://www.cards-lab.org/ecgvision-attrcm and AI-Echo: https://www.cards-lab.org/aiecho-attrcm). Executable applications of the AI-ECG and AI-TTE models can be made available for research use by contacting the corresponding author.

REFERENCES

1. Writing Committee, Kittleson MM, Ruberg FL, Ambardekar AV, Brannagan TH, Cheng RK, et al. 2023 ACC Expert Consensus Decision Pathway on Comprehensive Multidisciplinary Care for the Patient With Cardiac Amyloidosis: A Report of the American College of Cardiology Solution Set Oversight Committee. *J Am Coll Cardiol* 2023;**81**:1076–1126.

2. Tanskanen M, Peuralinna T, Polvikoski T, Notkola I-L, Sulkava R, Hardy J, et al. Senile systemic amyloidosis affects 25% of the very aged and associates with genetic variation in alpha2-macroglobulin and tau: a population-based autopsy study. *Ann Med* 2008;**40**:232–239.

3. Scully PR, Treibel TA, Fontana M, Lloyd G, Mullen M, Pugliese F, et al. Prevalence of Cardiac Amyloidosis in Patients Referred for Transcatheter Aortic Valve Replacement. *J Am Coll Cardiol* 2018;**71**:463–464.

4. Castaño A, Narotsky DL, Hamid N, Khalique OK, Morgenstern R, DeLuca A, et al. Unveiling transthyretin cardiac amyloidosis and its predictors among elderly patients with severe aortic stenosis undergoing transcatheter aortic valve replacement. *Eur Heart J* 2017;**38**:2879–2887.

5. AbouEzzeddine OF, Davies DR, Scott CG, Fayyaz AU, Askew JW, McKie PM, et al. Prevalence of Transthyretin Amyloid Cardiomyopathy in Heart Failure With Preserved Ejection Fraction. *JAMA Cardiol* 2021;**6**:1267–1274.

6. González-López E, Gallego-Delgado M, Guzzo-Merello G, Haro-Del Moral FJ de, Cobo-Marcos M, Robles C, et al. Wild-type transthyretin amyloidosis as a cause of heart failure with preserved ejection fraction. *Eur Heart J* 2015;**36**:2585–2594.

7. Maurer MS, Schwartz JH, Gundapaneni B, Elliott PM, Merlini G, Waddington-Cruz M, et al. Tafamidis Treatment for Patients with Transthyretin Amyloid Cardiomyopathy. *N Engl J Med* 2018;**379**:1007–1016.

8. Gillmore JD, Judge DP, Cappelli F, Fontana M, Garcia-Pavia P, Gibbs S, et al. Efficacy and Safety of Acoramidis in Transthyretin Amyloid Cardiomyopathy. *N Engl J Med* 2024;**390**:132–142.

9. Fontana M, Berk JL, Gillmore JD, Witteles RM, Grogan M, Drachman B, et al. Vutrisiran in patients with transthyretin amyloidosis with cardiomyopathy. *N Engl J Med* Massachusetts Medical Society; 2024.

10. Maurer MS, Kale P, Fontana M, Berk JL, Grogan M, Gustafsson F, et al. Patisiran Treatment in Patients with Transthyretin Cardiac Amyloidosis. *N Engl J Med* 2023;**389**:1553–1565.

11. Benson Merrill D., Waddington-Cruz Márcia, Berk John L., Polydefkis Michael, Dyck Peter J., Wang Annabel K., et al. Inotersen Treatment for Patients with Hereditary Transthyretin Amyloidosis. *N Engl J Med*; 2018;**379**:22–31.

12. Garcia-Pavia Pablo, aus dem Siepen Fabian, Donal Erwan, Lairez Olivier, van der Meer Peter, Kristen Arnt V., et al. Phase 1 Trial of Antibody NI006 for Depletion of Cardiac Transthyretin Amyloid. *N Engl J Med*; 2023;**389**:239–250.

13. Ioannou A, Patel RK, Razvi Y, Porcari A, Sinagra G, Venneri L, et al. Impact of Earlier Diagnosis in Cardiac ATTR Amyloidosis Over the Course of 20 Years. *Circulation* 2022;**146**:1657–1670.

14. Spielvogel CP, Haberl D, Mascherbauer K, Ning J, Kluge K, Traub-Weidinger T, et al. Diagnosis and prognosis of abnormal cardiac scintigraphy uptake suggestive of cardiac amyloidosis using artificial intelligence: a retrospective, international, multicentre, cross-tracer development and validation study. *Lancet Digit Health* 2024;**6**:e251–e260.

15. Dorbala S, Ando Y, Bokhari S, Dispenzieri A, Falk RH, Ferrari VA, et al. ASNC/AHA/ASE/EANM/HFSA/ISA/SCMR/SNMMI Expert Consensus Recommendations for Multimodality Imaging in Cardiac Amyloidosis: Part 1 of 2-Evidence Base and Standardized Methods of Imaging. *Circ Cardiovasc Imaging* 2021;**14**:e000029.

16. Ladefoged B, Dybro A, Povlsen JA, Vase H, Clemmensen TS, Poulsen SH. Diagnostic delay in wild type transthyretin cardiac amyloidosis - A clinical challenge. *Int J Cardiol* 2020;**304**:138–143.

17. Holste G, Oikonomou EK, Mortazavi BJ, Coppi A, Faridi KF, Miller EJ, et al. Severe aortic stenosis detection by deep learning applied to echocardiography. *Eur Heart J* 2023;**44**:4592-4604

18. Sangha V, Nargesi AA, Dhingra LS, Khunte A, Mortazavi BJ, Ribeiro AH, et al. Detection of Left Ventricular Systolic Dysfunction From Electrocardiographic Images. *Circulation* 2023;**148**:765-777.

19. Sangha V, Khunte A, Holste G, Mortazavi BJ, Wang Z, Oikonomou EK, et al. Biometric contrastive learning for data-efficient deep learning from electrocardiographic images. *J Am Med Inform Assoc* 2024;**31**:855-865

20. Sangha V, Mortazavi BJ, Haimovich AD, Ribeiro AH, Brandt CA, Jacoby DL, et al. Automated multilabel diagnosis on electrocardiographic images and signals. *Nat Commun* 2022;**13**:1583.

21. Sangha V, Oikonomou EK, Khera R. Artificial Intelligence Applied to Electrocardiographic Images for Scalable Screening of Transthyretin Amyloid Cardiomyopathy. medRxiv. 2024. p. 2024.09.30.24314651.

22. Coelho T, Dispenzieri A, Grogan M, Conceição I, Waddington-Cruz M, Kristen AV, et al. Patients with transthyretin amyloidosis enrolled in THAOS between 2018 and 2021 continue to experience substantial diagnostic delay. *Amyloid* 2023;**30**:445–448.

23. Ioannou A, Cappelli F, Emdin M, Nitsche C, Longhi S, Masri A, et al. Stratifying Disease Progression in Patients With Cardiac ATTR Amyloidosis. *J Am Coll Cardiol* 2024;**83**:1276–1291.

24. Rauf MU, Hawkins PN, Cappelli F, Perfetto F, Zampieri M, Argiro A, et al. Tc-99m labelled bone scintigraphy in suspected cardiac amyloidosis. *Eur Heart J* 2023;**44**:2187–2198.

25. Bokhari S, Castaño A, Pozniakoff T, Deslisle S, Latif F, Maurer MS. 99mTc-Pyrophosphate Scintigraphy for Differentiating Light-Chain Cardiac Amyloidosis From the Transthyretin-

Related Familial and Senile Cardiac Amyloidoses. *Circ Cardiovasc Imaging*; 2013;**6**:195–201.

26. Duffy G, Cheng PP, Yuan N, He B, Kwan AC, Shun-Shin MJ, et al. High-Throughput Precision Phenotyping of Left Ventricular Hypertrophy With Cardiovascular Deep Learning. *JAMA Cardiol* 2022;**7**:386–395.

27. Goto S, Mahara K, Beussink-Nelson L, Ikura H, Katsumata Y, Endo J, et al. Artificial intelligence-enabled fully automated detection of cardiac amyloidosis using electrocardiograms and echocardiograms. *Nat Commun* 2021;**12**:2726.

28. Grogan M, Lopez-Jimenez F, Cohen-Shelly M, Dispenzieri A, Attia ZI, Abou Ezzedine OF, et al. Artificial Intelligence-Enhanced Electrocardiogram for the Early Detection of Cardiac Amyloidosis. *Mayo Clin Proc* 2021;**96**:2768–2778.

29. Witteles RM, Bokhari S, Damy T, Elliott PM, Falk RH, Fine NM, et al. Screening for transthyretin amyloid cardiomyopathy in everyday practice. *JACC Heart Fail*; 2019;**7**:709–716.

30. Damrauer SM, Chaudhary K, Cho JH, Liang LW, Argulian E, Chan L, et al. Association of the V122I Hereditary Transthyretin Amyloidosis Genetic Variant With Heart Failure Among Individuals of African or Hispanic/Latino Ancestry. *JAMA* 2019;**322**:2191–2202.

31. Selvaraj S, Claggett BL, Quarta CC, Yu B, Inciardi RM, Buxbaum JN, et al. Age Dependency of Cardiovascular Outcomes With the Amyloidogenic pV142I Transthyretin Variant Among Black Individuals in the US. *JAMA Cardiol* 2023;**8**:784–788.

32. Selvaraj S, Claggett B, Shah SH, Mentz RJ, Khouri MG, Manichaikul AW, et al. Cardiovascular Burden of the V142I Transthyretin Variant. *JAMA* 2024;**331**:1824–1833.

33. Kittleson MM, Maurer MS, Ambardekar AV, Bullock-Palmer RP, Chang PP, Eisen HJ, et al. Cardiac Amyloidosis: Evolving Diagnosis and Management: A Scientific Statement From the American Heart Association. *Circulation* 2020;**142**:e7–e22.

34. Soman P, Garcia-Pavia P, Gillmore JD, Adams D, Conceicao I, Coelho T, et al. Rationale & design of ACT-EARLY, the acoramidis transthyretin amyloidosis prevention trial: Early detection using cardiac radionuclide imaging. *J Nucl Cardiol*; 2024;**38**:101948.

35. Spencer-Bonilla G, Njoroge JN, Pearson K, Witteles RM, Aras MA, Alexander KM. Racial and ethnic disparities in transthyretin cardiac amyloidosis. *Curr Cardiovasc Risk Rep*; 2021;**15**.

TABLES

Table 1 | Participant-level demographics for progression analysis.

		YNHHS (internal)		HMH (external)	
Nuclear cardiac amyloid imaging status		**Negative**	**Positive**	**Negative**	**Positive**
Total participants (n)		872	112	632	174
Age at nuclear cardiac amyloid imaging (years)		73 [64, 80]	82 [75, 86]	67 [57-75]	77 [70-82]
Sex	*Female*	401 (46.0)	35 (31.3)	249 (39.4)	29 (16.7)
	Male	471 (54.0)	77 (68.8)	383 (60.6)	145 (83.3)
Race	*Asian*	7 (0.8)	0 (0)	11 (1.7)	3 (1.7)
	Black	245 (28.1)	31 (27.7)	279 (44.1)	70 (40.2)
	White	577 (66.3)	77 (68.8)	324 (51.3)	97 (55.7)
	Other	26 (3.0)	2 (1.8)	11 (1.7)	2 (1.2)
	Unknown	17 (1.9)	2 (1.8)	7 (1.1)	2 (1.2)
Ethnicity	*Hispanic*	32 (3.7)	6 (5.4)	54 (8.5)	8 (4.6)
	Non-Hispanic	819 (93.9)	105 (93.8)	576 (91.1)	163 (93.7)
	Unknown	21 (2.4)	1 (0.9)	2 (0.3)	3 (1.7)
Conditions	*Hypertension*	804 (92.3)	107 (95.5)	605 (95.7)	161 (92.5)
	Diabetes Mellitus	388 (44.5)	34 (30.4)	298 (47.2)	50 (28.7)
	Chronic Kidney Disease	352 (40.4)	42 (37.5)	442 (69.9)	113 (64.9)
	Any Heart Failure	593 (68.1)	86 (76.8)	510 (80.7)	147 (84.5)
	Any cardiomyopathy	403 (46.3)	50 (44.6)	357 (56.5)	121 (69.5)
Participants in the TTE sub-study		872 (100)	112 (100)	551 (87.2)	144 (82.8)
TTE study count per patient		3 [2, 5]	3 [2, 6]	8 [5-13]	6 [3-10]
Participants in the ECG sub-study		857 (98.3)	71 (63.3)	632 (100)	174 (100)
ECG study count per patient		17 [7, 32]	11 [4, 21]	9 [4-17]	7 [3-13]

Summary statistics are presented as counts (n) with valid percentages (%) or median [25th 75th percentile]. ECG: electrocardiography; HMH: Houston Methodist Hospital; TTE: transthoracic echocardiography; YNHHS: Yale-New Haven Health System.

Table 2 | Association between nuclear cardiac amyloid testing positivity, time, age, and sex with longitudinal AI-Echo and AI-ECG probabilities of ATTR-CM.

	Yale-New Haven Health System (YNHHS)		Houston Methodist Hospitals (HMH)	
	AI-Echo (n=984 patients)	**AI-ECG (n=928 patients)**	**AI-Echo (n=695 patients)**	**AI-ECG (n=806 patients)**
Nuclear cardiac amyloid test positivity (positive, vs negative)	0.25 [0.22-0.27], *p*<0.001	0.13 [0.10-0.16], *p*<0.001	0.22 [0.20-0.25], *p*<0.001	0.13 [0.10-0.15], *p*<0.001
Age at nuclear cardiac amyloid testing (per 10-year incr.)	0.00 [-0.01, 0.01], *p*=0.64	0.02 [0.02-0.03], *p*<0.001	-0.01 [-0.01, 0.00], *p*=0.14	0.02 [0.01-0.02], *p*=0.001
Sex (male, vs female)	-0.01 [-0.02-0.01], *p*=0.63	0.05 [0.03-0.06], *p*<0.001	0.02 [0.00-0.05], *p*=0.027	0.06 [0.03-0.08], *p*<0.001
Time between study and nuclear cardiac amyloid testing (per 10-year incr.)	0.07 [0.05-0.09], *p*<0.001	0.07 [0.06-0.09], *p*<0.001	0.03 [0.01-0.05], *p*=0.001	0.10 [0.07-0.13], *p*<0.001
Interaction between nuclear cardiac amyloid testing positivity *x* time	**0.16 [0.11-0.22], *p*<0.001**	**0.08 [0.05-0.10], *p*<0.001**	**0.15 [0.10-0.20], *p*<0.001**	**0.08 [0.03-0.13], *p*=0.004**

Results from mixed linear regression models with AI-derived ATTR-CM probabilities (0 through 1) as the dependent variable, nuclear cardiac amyloid testing status (positive versus negative), age at nuclear cardiac amyloid testing testing, sex, time difference between echocardiography (or ECG) and nuclear cardiac amyloid testing, an interaction term for time versus nuclear cardiac amyloid testing status as independent fixed effects, and participant included as a random effect. ATTR-CM: transthyretin amyloid cardiomyopathy; ECG: electrocardiography.

FIGURE LEGENDS

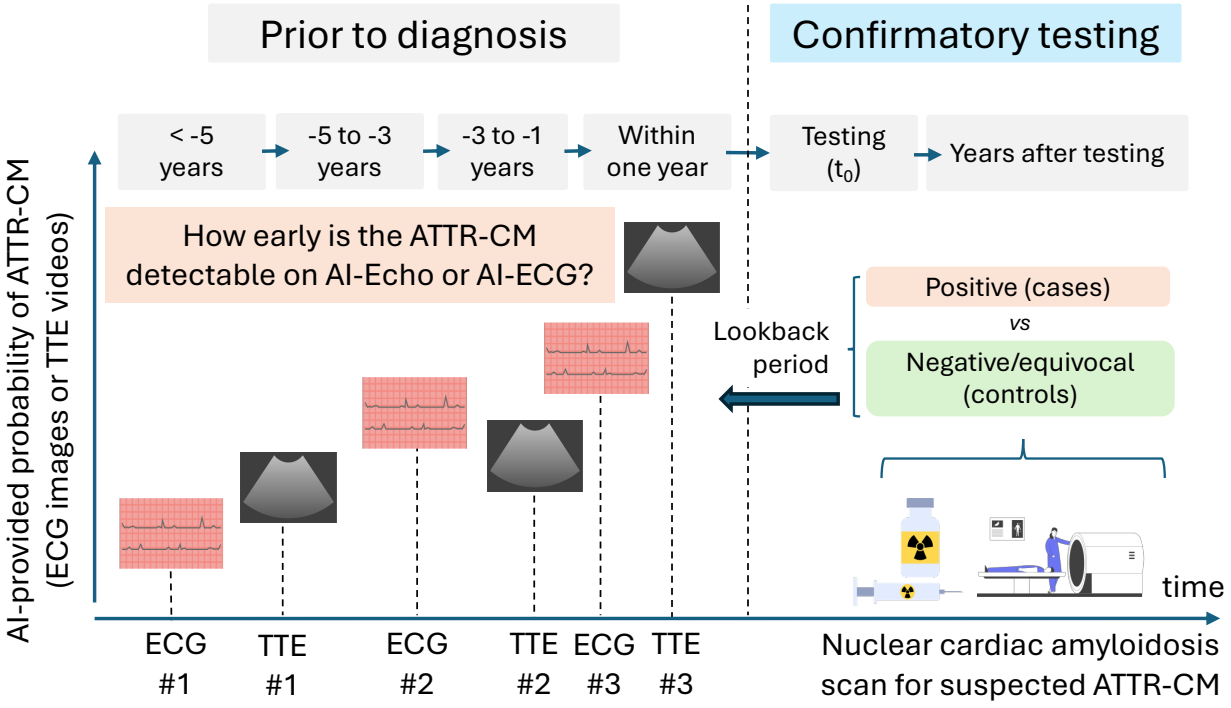

Figure 1 | Study Population. Deep learning algorithms were trained to discriminate nuclear cardiac amyloid imaging-positive cases of ATTR-CM from age- and sex-matched controls using standard TTE videos or ECG images. These were subsequently deployed across independent sets of patients with longitudinal monitoring by TTE or ECG pre-dating their referral for nuclear cardiac amyloid testing. The overall objective was to examine the ability of the AI models to detect changes in TTE or ECG signatures that precede clinical disease and diagnosis. Such AI-enabled TTE or ECG signatures may be used to forecast the development of ATTR-CM, thus offering a standardized and scalable platform for longitudinal monitoring and screening in the community. AI: artificial intelligence; ATTR-CM: transthyretin amyloid cardiomyopathy; ECG: electrocardiography; Tc^{99m}-PYP: pyrophosphate; TTE: transthoracic echocardiography.

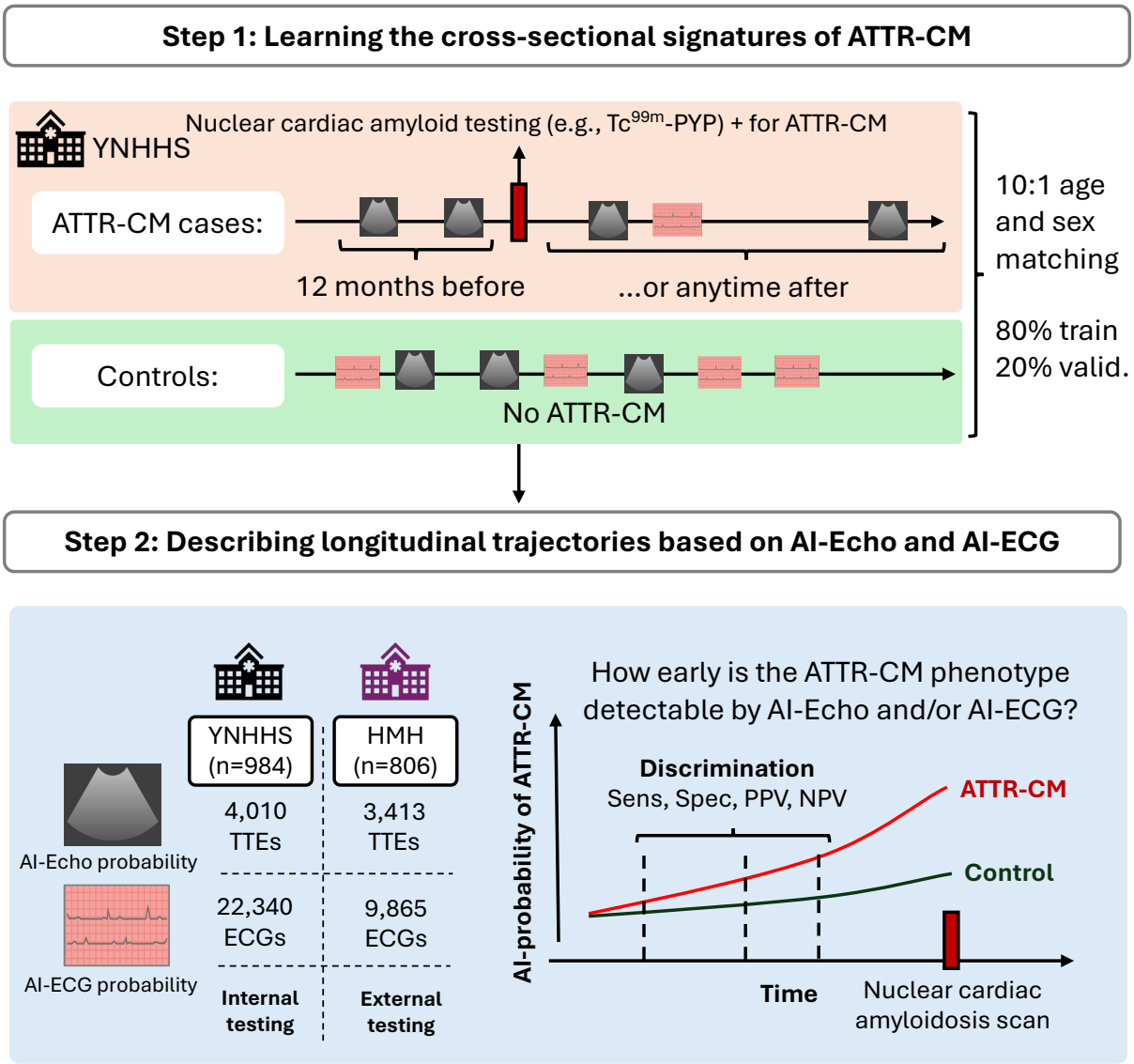

Figure 2 | Study Design. AI-models were trained on transthoracic echocardiograms (TTE) and 12-lead electrocardiographic (ECG) images from patients with ATTR-CM (based on a positive nuclear cardiac amyloid test performed no more than 12 months after the index study) as well as age- and sex-matched controls without known disease across the Yale-New Haven Health System (YNHHS). Models were subsequently deployed across independent sets of patients in YNHHS, as well as an external set of patients from Houston Methodist Hospitals (HMH) who had sequential TTE or ECG performed in the years leading up to their referral for nuclear cardiac

amyloid imaging. This design allowed us to evaluate the progression of AI-Echo or AI-ECG probabilities as non-invasive markers of pre-clinical ATTR-CM progression. AI: artificial intelligence; ATTR-CM: transthyretin amyloid cardiomyopathy; ECG: electrocardiography; HMH: Houston Methodist Hospitals; Tc^{99m}-PYP: pyrophosphate; TTE: transthoracic echocardiography; YNHHS: Yale-New Haven Health System.

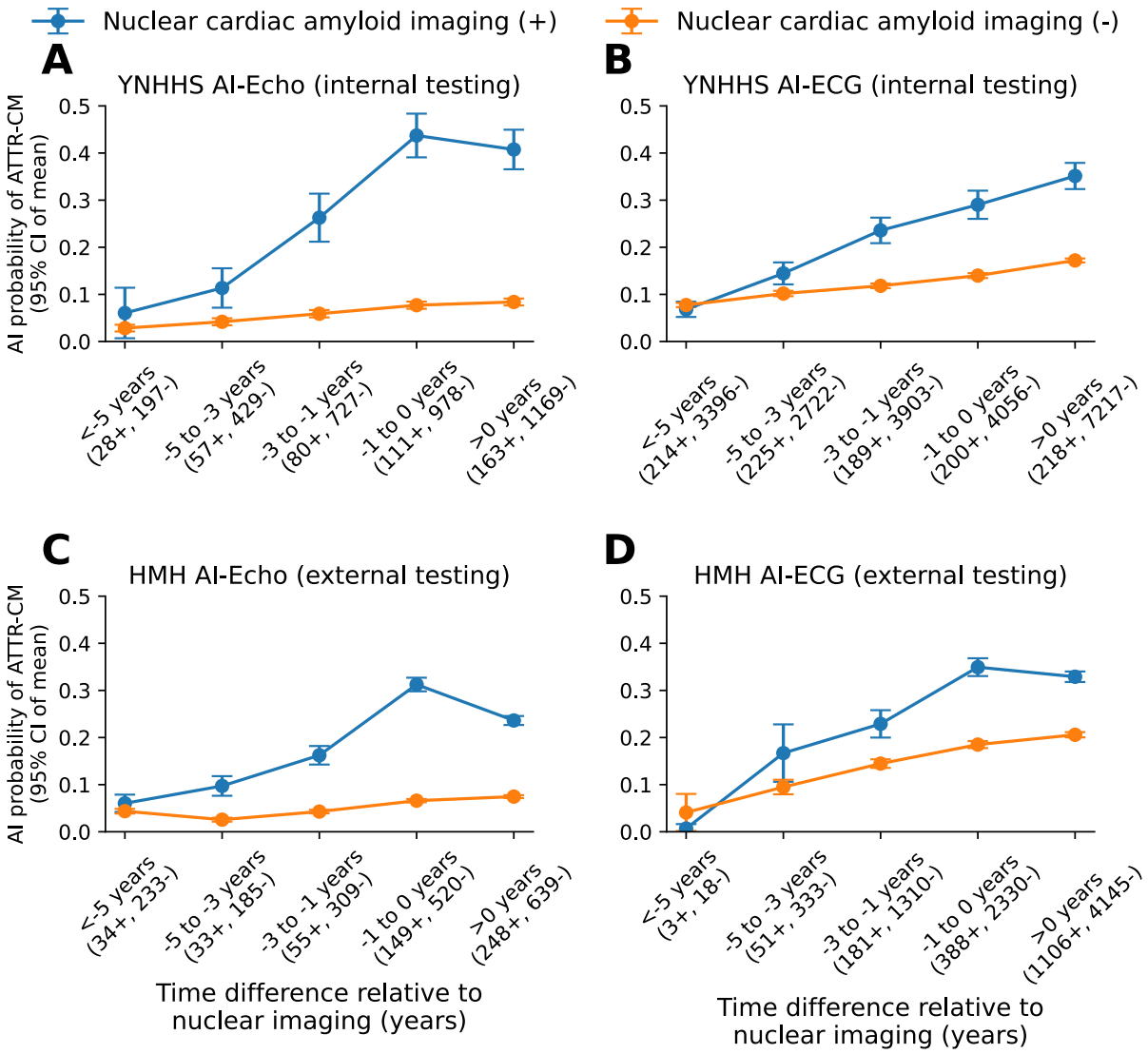

Figure 3 | Longitudinal changes in AI-Echo and AI-ECG ATTR-CM probabilities across cohorts and modalities stratified by eventual nuclear cardiac amyloid positivity. The panels illustrate the mean (with error bars denoting the 95% confidence interval of mean) of the AI-Echo and AI-ECG-derived probabilities in studies of patients who went on to have a positive (blue color) vs negative (orange color) nuclear cardiac amyloid test in YNHHS (*internal testing*: **A, B**) and HMH (*external testing*: **C, D**), respectively. The x axis denotes the time between the TTE/ECG and the timing of nuclear cardiac amyloid testing summarized across discrete time groups (negative time differences suggest that the TTE/ECG was performed before the nuclear

cardiology exam). The brackets below each time period denote the number of unique positive and negative studies. AI: artificial intelligence; ATTR-CM: transthyretin amyloid cardiomyopathy; ECG: electrocardiography; HMH: Houston Methodist Hospitals; TTE: transthoracic echocardiography; YNHHS: Yale-New Haven Health System.

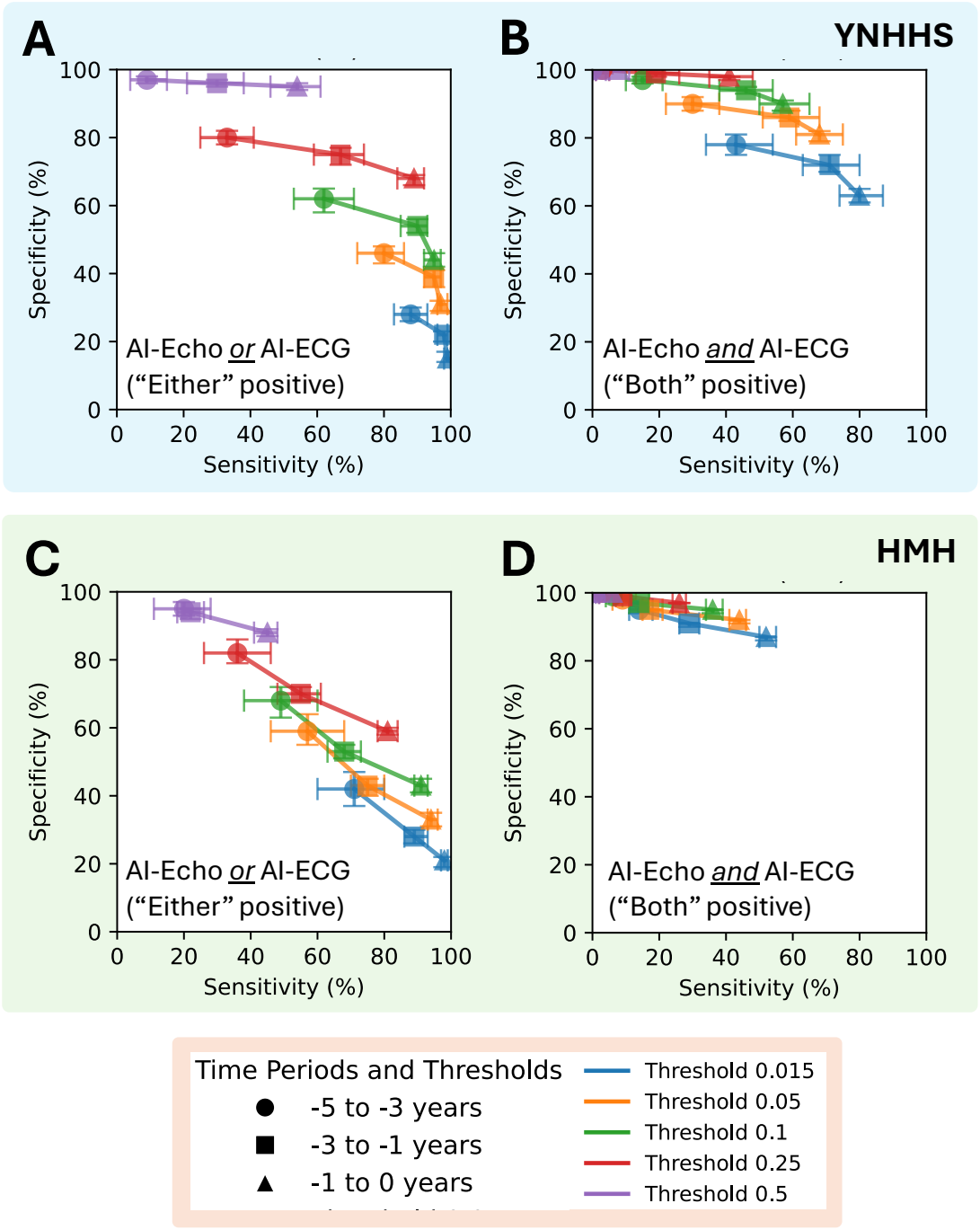

Figure 4 | Sensitivity and specificity of combined or parallel screening for ATTR-CM by AI-ECG and AI-Echo. Each plot represents the sensitivity and specificity at a given threshold (0.015: blue, 0.05: orange, 0.1: green, 0.25: red, 0.5: purple) and a given time point (circle: 5 to 3 years; rectangle: 3 to 1 year(s) before; and triangle: year before nuclear cardiac amyloid testing

across YNHHS (**A-B**) and HMH (**C-D**). The panels depict two different strategies: an "either" strategy (**A&C**: either one of the two modalities required to be positive), and a "both" strategy (**B&D**: both tests required to be positive). The error bars in either direction denote the 95% confidence intervals for sensitivity or specificity derived from bootstrapping with 1000 replications. ATTR-CM: transthyretin amyloid cardiomyopathy; ECG: electrocardiography; HMH: Houston Methodist Hospitals; TTE: transthoracic echocardiography; YNHHS: Yale-New Haven Health System.